Two Hundred Years of Capillarity Research

Two centuries after seminal work by Pierre-Simon Laplace and Thomas Young, capillarity's modern applications arise in fields ranging from biology and oceanography to propulsion, materials science, and novel devices.

Yves Pomeau and Emmanuel Villermaux

Capillarity is a manifestation of the cohesion of matter due to strong, short-ranged forces between adjacent particles. Examples abound: The curving meniscus in test tubes and the soaking up of liquids by a sponge reflect the balance between the adhesive forces between the walls and liquid and the cohesive forces or surface tension of the liquid. In fluids and other deformable media, capillary forces—a general term that encompasses adhesive and cohesive forces and surface tension—tend to minimize the surface area of a given volume and are responsible for the spherical shape of isolated drops. Although qualitatively straightforward to describe, capillary phenomena have presented numerous challenges to quantitative understanding.

The notion of force was central to the early development of modern physics. The foremost example was the gravitational force, by which large masses attract each other. Capillarity first arose in the history of ideas as an anomaly to the law of attraction: The action of capillary forces in a tube lifts a wetting fluid, a behavior that seemed to contradict the Aristotelian concept of a "natural" state of rest in which ponderous matter tries to reach as low a position as possible.

Capillary effects were puzzling a couple of bright and imaginative spirits at the Royal Society of London by the time of Isaac Newton, who himself mentions the phenomenon in query 31 of his *Opticks*.[1] Experiments by Francis Hauksbee and James Jurin that investigated the capillary rise between solid plates and in tubes clarified the effect: The mass of fluid raised is proportional to the distance between the plates. Newton assumed the vertical attraction was independent of the gap between the plates. Therefore the balance between the downward pull of gravity and the constant capillary attraction leads to the correct law of proportionality between the inverse of the gap and the vertical rise. Newton, however, did not clearly say why the vertical attraction is independent of the gap and why it should be proportional to the length of the contact line between the liquid and the solid. Those findings were from Jurin, for whom the law is named.

*Yves Pomeau is a CNRS senior researcher at the École Normale Supérieure's Laboratory of Statistical Physics in Paris. **Emmanuel Villermaux** is a professor at the Institute for Research on Non-equilibrium Phenomena at the Université de Provence in Marseille, France, and at the Institut Universitaire de France.*

A decisive step in the understanding of capillary phenomena occurred in 1805 with the publication of an essay by Thomas Young[2] and of a supplement by Pierre-Simon Laplace to the fourth volume of his treatise on celestial mechanics.[3] Those two contributions differ in their style: Young's is more qualitative, and Laplace's is more analytic. Indeed, as noted by John Rowlinson, "In reading Young we are reading 18th century natural philosophy; in reading Laplace we are reading 19th century theoretical physics."[4] The two works also emphasize quite different aspects of capillarity, which provide the general division of this article: Young is associated more closely with situations involving three thermodynamic phases—in particular, a vapor, a liquid, and a solid wall. Those situations would nowadays be gathered in a broad class under the rubric of wetting. Laplace, initially concerned with the determination of equilibrium shapes of free menisci and liquid bridges, is more closely associated with free surfaces.

Young, surface tension, and wetting

In his article on capillary action for the *Encyclopedia Britannica*,[4,5] James Clerk Maxwell wrote that Johann Andreas von Segner, a Hungarian mathematician, first developed the concept of surface tension, but Young is responsible for the bright idea of using that concept to explain various experimental observations in detail. The notion of surface tension relies on an analogy: The interface between a liquid and a vapor behaves like a membrane (see figure 1) under isotropic tension, a bit like a violin string under tension (although no mass per unit area can be attributed to a liquid–vapor interface). Because of that tension, the surface tends to reduce its area as much as it can under given boundary conditions and the constraint that the enclosed volume remains constant. Carl Friedrich Gauss later refined that point of view and put it in modern variational form.

Surface tension leads directly to the equilibrium contact angle where the three phases—usually, but not always, liquid (l), solid (s), and vapor (v)—meet. That angle, θ_{YL}, is given by the Young–Laplace (YL) relation $\sigma_{lv} \cos \theta_{YL} = \sigma_{ls} - \sigma_{vs}$, where σ is the surface tension of the interface between the two indicated phases.

The angle θ_{YL} is measured from the solid–liquid interface. If the value of $\cos \theta_{YL}$ predicted by the YL equation is less than −1, one has perfect wetting—the liquid coats the surface. If $\cos \theta_{YL}$ is greater than 1, one has perfect drying. The meeting or merging of three thermodynamic bulk phases (liquid-solid-vapor) occurs generically along a line, as do generally three volumes. Surprisingly, one of us (Pomeau) and colleagues have shown that four phases (two liquid, one solid, and one vapor) may also merge robustly along a line, a phenomenon yet to be observed.
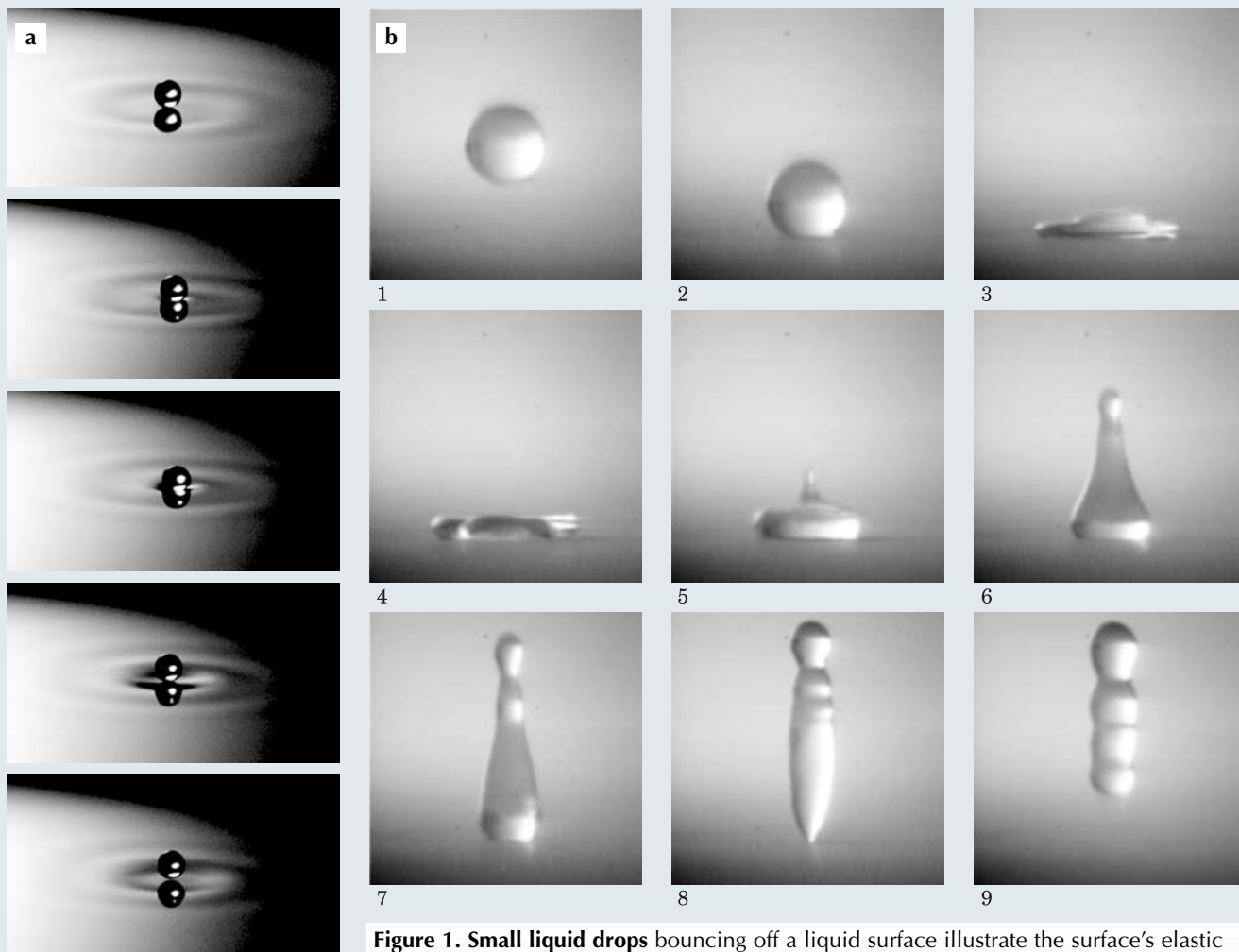
Figure 1. Small liquid drops bouncing off a liquid surface illustrate the surface's elastic membrane-like behavior. **(a)** For a low initial height, this submillimeter-diameter drop remains close to spherical. The images were taken every few milliseconds. (Courtesy of S. Protière and Y. Couder.) **(b)** For larger amplitudes, deformations can be strong. Here a water drop with an initial diameter of 2.5 mm and velocity of 0.83 m/s falls on a super-hydrophobic surface. The time interval between pictures is 2.7 ms. (Courtesy of C. Clanet, C. Beguin, D. Richard, and D. Quéré.)

The YL theory of the merging of a liquid–vapor interface with a solid does not apply directly to many physical situations, because most real solid surfaces are rough and heterogeneous due to all kinds of causes, including chemistry, crystal defects, and the like. That heterogeneity has long been known to be responsible for the phenomenon of contact-angle hysteresis: Most real liquid–solid contact angles at rest take arbitrary values within a certain range. The angles are also history dependent, not single valued as predicted by the YL formula. A consequence is the common observation that a droplet on an incline (a windshield, for instance) can remain at rest. The sensitivity of the contact angle to the heterogeneity of solid surfaces comes from the fact that, as the liquid–vapor interface crosses the solid surface, the interface is so thin (of molecular thickness, except near the critical point) that it probes the solid at very small scales and does not average its surface properties well.

From statics to dynamics

An even tougher question is how to extend the YL equilibrium theory to dynamical phenomena, such as when a droplet slides on an incline with or without contact-angle hysteresis. The only case in which this problem is well understood is the rolling of a droplet of nonwetting fluid (for instance, mercury on plastic). If such a droplet is substantially smaller than the capillary length $\sqrt{\sigma_{lv}/\rho g}$, the length—a few millimeters for ordinary liquids under normal gravity conditions—below which capillary forces dom-

inate over gravitational forces, the droplet's shape is close to spherical except for a small contact disk on the solid. (Here, ρ denotes the liquid density and g the acceleration of gravity.) When the solid is tilted, the droplet rolls down. Theory and experiment agree that the droplet rolls down with a constant shape, almost like a solid sphere, in a rolling or cycloidal motion.[6] Things become more tricky if, at equilibrium, the droplet merges with the solid at a finite contact angle θ_{YL}, different from 0 (no wetting) and π (perfect wetting).

Consider a vapor–liquid contact line that slides on a solid surface, with U the component of the velocity perpendicular to the orientation of the interface. By a formally simple extension of the YL formula, one can relate the contact angle θ to U through a mobility relation $U = f(\theta, \theta_{YL})$. The function f satisfies $f(\theta_{YL}, \theta_{YL}) = 0$; the contact angle matches the YL value only when the interface is at rest. At low speeds—that is, for a small dimensionless capillary number $Ca = \eta U/\sigma_{lv}$, where η is the liquid viscosity—the viscous stress is negligible compared to capillary stress, and there is a well-defined method, once f is known, for computing the shape and velocity of descent of a droplet on an incline. For a given shape of the contact line and a given volume of liquid, one computes the shape of the surface that minimizes the area. Along the perimeter where
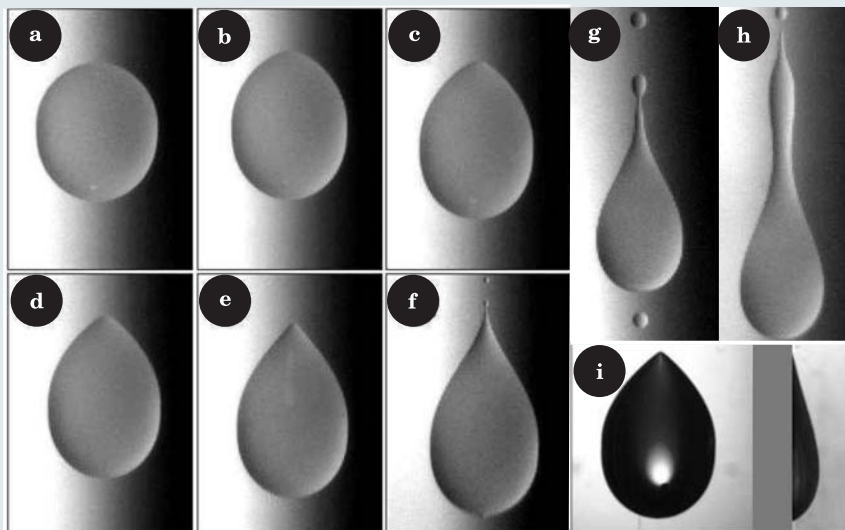
Figure 2. Drops sliding down a plane under conditions of partial wetting. At low velocity, the drop is rounded **(a)**; as the velocity increases **(b–d)**, the drop develops a singularity at the rear where the two sides meet. At even higher velocity, the singularity evolves toward a cusp **(e)** and to different regimes of pearling **(f–h)** in which smaller static droplets are left behind the main drop. **(i)** Top and side views showing the singular nature of the interface that first occurs in **(d)**, sometimes called the corner regime. (Courtesy of T. Podgorski, J.-M. Flesselles, A. Daerr, N. Le Grand-Piteira, and L. Limat.)

the drop meets the surface, one obtains a value of θ that can be used in the mobility relation. The result is the instantaneous speed of the perimeter, which leads to an elementary displacement along the solid surface, from which the evolved drop geometry can be determined.

With a linear mobility relation $U = k(\theta - \theta_{YL})$, one can work out the case of a shallow droplet sliding on an incline at constant speed. Below a certain speed, the contact perimeter is a circle, and it becomes cusped in the back beyond the critical value U_{cr} for which the contact angle is 0: $U_{cr} = f(\theta = 0, \theta_{YL})$. That condition is first met on the sliding drop's back perimeter, where some sort of dynamical wetting transition occurs (figure 2).

Including the viscous stress in that picture is difficult and not well understood. There is not yet a satisfactory solution to the problem of a moving contact line. Consider a wedge of fluid sliding on a solid plane. If the usual no-slip condition is satisfied by the liquid flowing along the solid, the liquid-vapor-solid interface cannot be a material line, that is, a line following the local fluid speed! Either there is some evaporation and condensation near the contact line, to break the condition that the liquid–vapor interface is a material surface, or there must be a little bit of sliding permitted near the solid surface.[7] The effect of viscous stresses in the moving cusp problem has been recently examined by the groups of Laurent Limat, Howard Stone, and one of us (Pomeau).[8]

Although capillary phenomena are relevant mostly for the surface of liquids in contact with their vapor, they are also significant for defining the shape of crystals. The crystal–vapor surface tension depends on the local orientation of the surface with respect to the crystal axis. At equilibrium, flat facets are found when surface tension has a discontinuous gradient with respect to the orientation. In most cases, the actual shape of crystals reflects the history of their growth, because their shape's relaxation to equilibrium is too slow to be effective: It requires the migration of atoms along the surface itself, a much slower process than that of relaxation by mass transfer inside a fluid approaching equilibrium. However, there are beautiful illustrations of equilibrium shapes of liquid crystals with the ability to flow, such as the ordered, so-called blue phase of cholesterics (figure 3).

More complex wetting

The interaction between thin coating films and the solid surface underneath may depend in a complex manner on the film thickness. This has important consequences for the shape of tiny droplets of polymer spreading on a solid.[9] Because of thickness-dependent interactions, a film of initially small thickness may present instabilities that lead to dewetting or to the generation of regular patterns at micron or nanometer scales. Such effects are presently being considered for building devices in micro- and nanoelectronics. A fairly recent field of research in dynamical wetting phenomena is related to various additional effects associated with the dependence of surface tension on such factors as electric fields, added chemicals, or temperature. Those effects can be used to control the movement of small volumes of fluids (see PHYSICS TODAY, May 2004, page 9).[9]

Solid substrates with periodic roughness—either natural or fabricated—in the micron range may introduce new capillary effects. In 1936, Robert Wenzel explained such
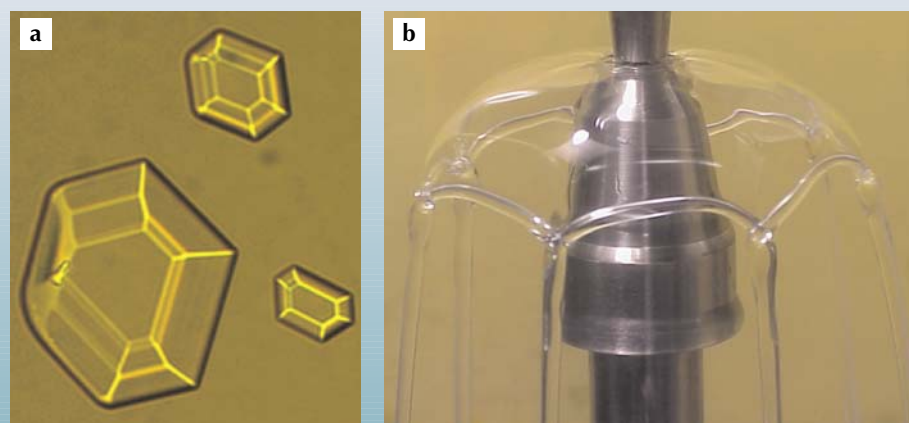
Figure 3. Surface tension can create sharp edges and corners in some systems. **(a)** Faceted liquid crystals in a mixture of monoolein and water. (Courtesy of Pawel Pieranski.) **(b)** A liquid umbrella formed by the impact of a jet of a water–glycerin solution, 50 times more viscous than pure water, on a solid surface. The resulting liquid sheet has a cusped rim due to an instability caused by surface tension. (Courtesy of J. Bush.)

Figure 4. A millimeter-sized water drop at the surface of a textured substrate. The substrate is practically dry even though it supports the drop weight. The regularity of the substrate grooves is evident from its ability to diffract white light. (Courtesy of M. Callies and D. Quéré.)

effects by modifying Young's formula, scaling the $\cos \theta$ term by the ratio of the actual surface area to the plane surface area to account for surface roughness. Those so-called textured surfaces may sometimes be super-hydrophobic—that is, strongly nonwetting, as shown in figure 4. A famous natural example is the lotus leaf, which remains dry and clean in the rain and is thus able to maintain evaporation of sap on its surface and therefore the flow of nutrients in the plant stem. Superhydrophobicity may have interesting technological applications, such as future self-cleaning glasses and windshields.

Laplace and free-surface shapes

Laplace's fundamental and decisive contribution to the field was to quantify the interplay between the interface geometry and the stress it sustains. Consider an interface whose principal radii of curvature—that is, minimum and maximum radii of curvature—are R_1 and R_2. The total curvature κ is then defined to be $\kappa \equiv 1/R_1 + 1/R_2$. Assuming, with no direct proof at the time, a short-range attractive force between fluid "molecules," Laplace reasoned that the pressure difference Δp across a liquid–vapor interface is related to the interface curvature through $\Delta p = \sigma_{lv} \kappa$. That relationship allowed him to solve a number of static problems, like the shape of menisci. Writing 70 years later, Maxwell described Laplace's contribution as "an example which has never been surpassed."[5]

Laplace did not explicitly use surface tension at the start, but instead assumed a short-range interaction between homogeneous, space-filling fluid elements and deduced an effective surface tension. It was understood progressively throughout the 19th century that the interaction range is on the order of the size of the atoms. Specifically, for a system at temperature T, the surface tension is on the order of the thermal energy density $k_B T/l^3$ times the liquid's interatomic distance l, so that $\sigma_{lv} \approx k_B T/l^2$, about 10^{-1} N/m for simple liquids at room temperature (for which $l \approx 10^{-10}$ m). The surface tension of water is somewhat greater because of hydrogen bonds—ionically strong, long-range forces. In the neighborhood of the liquid–vapor transition, where the two thermodynamic phases are nearly identical, surface tension vanishes. Laplace also assumed a sharp discontinuity of density at the liquid–vapor interface. That idealization has since been replaced, following a remark by Siméon-Denis Poisson and later work by Maxwell and Johannes van der Waals, by a more realistic picture of a smooth density change.

Breakup and fragmentation

The overall trend on the free-surface side of capillarity research has been a shift from static shapes to the dynamics of free-surface flows, breakup, and fragmentation. An obvious manifestation of capillarity is the formation of drops from the rupture of liquid threads, ligaments, and jets, as illustrated in figure 5. The smooth, uniform long liquid cylinder has become the paradigm of droplet formation.

Following early observations by Edme Mariotte and Félix Savart that a liquid jet eventually ends in a train of droplets,[10] subsequent studies first explained *why* the basic smooth state is unstable.[11] The answer arises from a peculiar property of cylinders: When slightly distorted in a peristaltic (axisymmetric) fashion at constant volume, they present a smaller surface area than the original area of the straight cylinder, at least for a range of longitudinal perturbations whose longitudinal wavelength is larger than the circumference of the cylinder. Capillary forces, which drive the cylinder toward the configuration that minimizes its net area, thus cause an instability. The axisymmetric form of Laplace's law, for a body of rotational symmetry with a local radius $r(z)$, states that

$$\Delta p = \sigma_{lv} \left(\frac{1}{r(1 + r'^2)^{1/2}} - \frac{r''}{(1 + r'^2)^{3/2}} \right),$$

where $r' = dr/dz$.

Using this expression and the dynamical response of the liquid from fluid mechanics, Lord Rayleigh[12] addressed the next natural question, namely, how quickly the instability develops. Capillary forces move fluid particles apart along

Figure 5. Drop formation in ligaments. Two jets, normal to the page and meeting at a 72° angle, make a thin liquid sheet, the rim of which is visible here. The 10 panels on the right show the evolution of the fragmentation at the section of the rim indicated by the dashed blue line on the left; the arrows trace a ligament along the rim as it evolves. The time interval between the panels is 1 ms. The average shape of the sheet follows Laplace's law applied to its free edges.[18]

5 mm
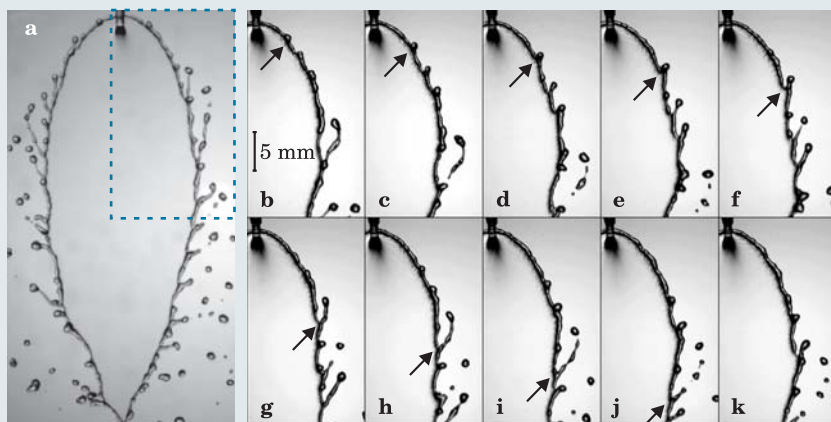
the thread; for a thread of diameter d and density ρ, the time scale τ balancing inertial forces $\rho d^3 \times d/\tau^2$ and capillary forces $\sigma_{lv} d$ is given by

$$\tau \sim \sqrt{\frac{\rho d^3}{\sigma_{lv}}},$$

and is on the order of 10^{-2} s for a millimeter-diameter jet. Viscous slowing was soon included in the analysis, and the impact of surface tension on a number of dynamical problems in fluids, such as capillary waves and gravitational destabilization of stratified flows, was understood by Rayleigh's time.

The thread finally disrupts into disjoint drops, and recent studies focusing on that very final stage of the instability, led in particular by Jens Eggers,[13] have discovered how. Close to the final singularity, the still-connected thread has a double-cone shape, with the cones touching at their summits (figure 6). The angles of the cones are not the same, but they are fully determined from a particular solution of the nonlinear equations of motion (the solution lasts for about 10^{-3} of the overall unstable time scale τ). That universal, singular evolution persists for tiny threads, such as nanojets, affected by thermal Brownian noise, although they break in a symmetric fashion.[14]

While 19th-century research focused on the nature of the instability around the unperturbed state, recent work has emphasized the nonlinear, universal character of the ultimate stages of breakup in threads. The phenomenon is also altered in an essential way in non-Newtonian, shear-thinning fluids with polymers (figure 6b) and in the presence of surfactants. Modification of the instability due to confinement by solid walls has also been recently reexamined in a particular technological context: Most microfluidic device channels are rectangular, and often more two-dimensional than axisymmetric. Those small devices also offer the useful feature of controlling breakup in such a way that the resulting drops are almost uniformly sized, a useful property for preparing various emulsions or encapsulation.[9]

Sprays and foams

Natural or manmade sprays are characterized by broad distributions of the drops' sizes. That aspect of spray formation
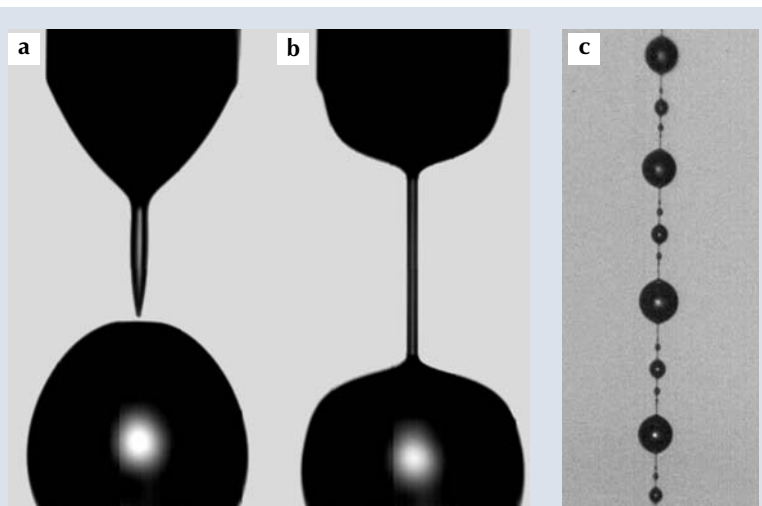
Figure 6. Filament breakup. (a) Drop formation for pure water. The self-similar dynamics of the thinning filament is given by a balance between capillary and inertial forces. **(b)** The exact same experiment, but with 0.1 g/L of a long, flexible polymer added to the water. The dynamics is completely changed, and a long filament forms between the orifice and the drop. The new dynamics is due to the enormous resistance to elongational (stretching) flows of dilute polymer solutions. (Courtesy of Y. Amarouchene, D. Bonn, J. Meunier, and H. Kellay.) **(c)** The late stage of the filament breakup. These "beads on a string" formed from iterated instabilities in a polyethylene oxide solution in water. (Courtesy of M. Oliveira and G. McKinley.)

affects both industrial and geophysical applications—it comes into play in liquid-propulsion combustion chambers and diesel engines and is a salient facet of rainfall and spume formed by the wind over the ocean. Aerosols formed from the bursting of bubbles at the surface of the sea (figure 7) contribute notably to exchange with the atmosphere. Understanding the size distributions is a typical modern problem, as it combines complicated microscopic phenomena with nontrivial, and often broad, global statistics.

Little is known in detail about the reasons for the broad statistics, although one of us (Villermaux) has suggested, and provided some experimental evidence, that a coalescence-like effect within the ligaments themselves while they break is responsible for the size polydispersity of the resulting spray.[15] Unstable capillary waves traveling along the ligament overlap as the ligament's constitutive
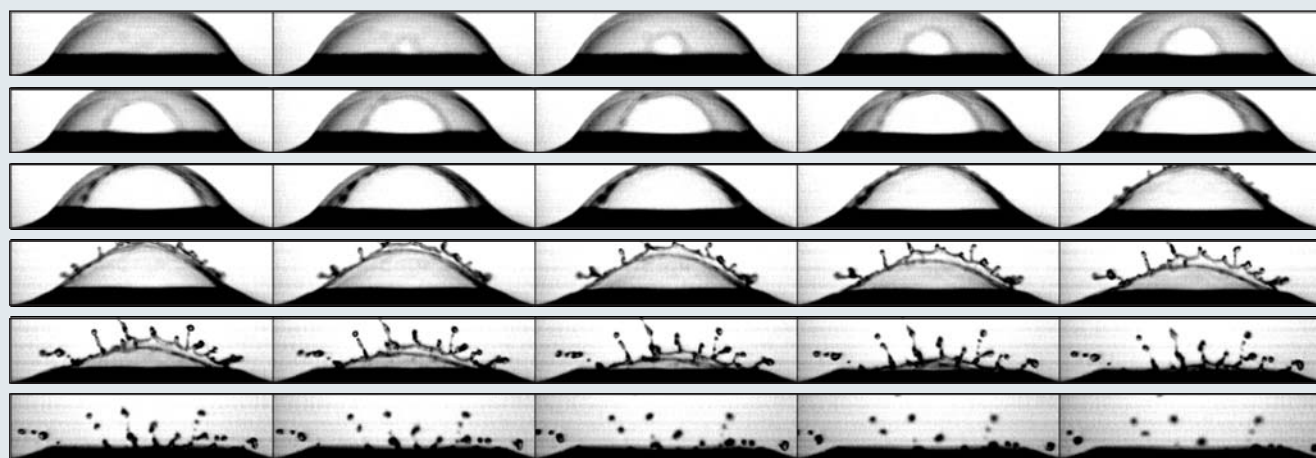
Figure 7. A bubble about 2 cm in diameter stands at the surface of a quiescent liquid. The bubble nucleates a hole that opens due to the unbalanced capillary forces at its edge. The liquid collected at the rim gets centrifuged and destabilizes to form ligaments and then drops.
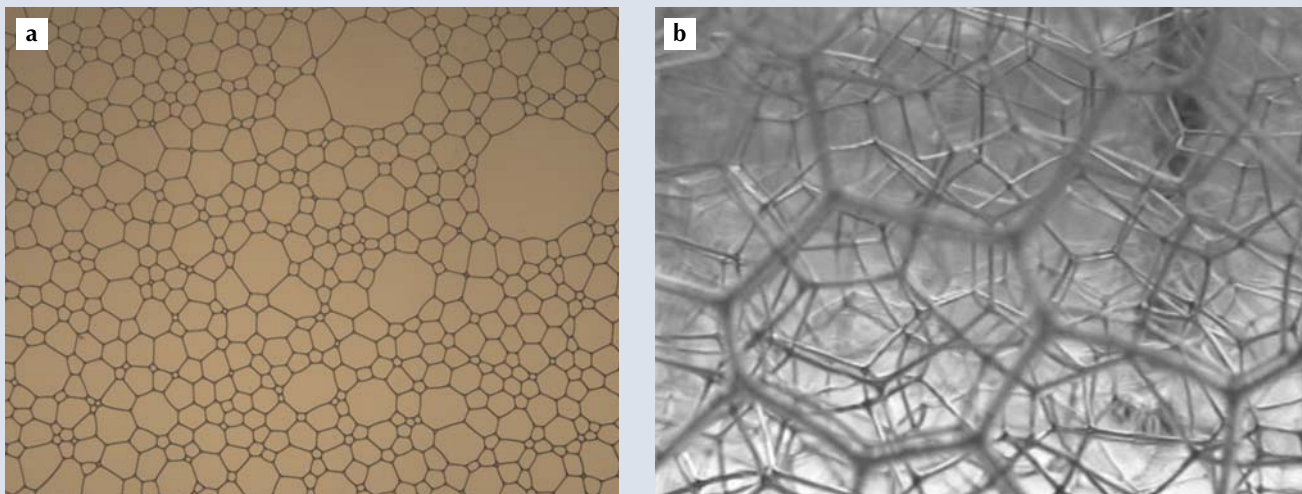
Figure 8. As foams age, they coarsen, and the average cell size increases. **(a)** A coarsening foam in two dimensions. The rate of change of a cell area depends on its number of sides, as described by John von Neumann.[16] **(b)** A 3D soap foam, which is slowly draining inside a square container. Many layers of interconnected cells are visible. The liquid is 75% water, 20% glycerin, and 5% dishwashing soap. The horizontal extent of the image is about 2 cm. Huge cells coexist with tiny ones; determining the distribution of cell surfaces and volumes while the foam coarsens remains a subject of active research. (Figure 8b courtesy of E. Tan and S. Thoroddsen.)

liquid volumes separate, and end up producing larger drops. Thus the shape of the size distribution is, surprisingly, determined by aggregation, rather than by the frequently held view of a cascading sequence of breakups.

Foams stabilized by surfactants play an important technological role, such as in ore-dust recovery. The understanding of the structure of liquid foams and of the dynamics of their coarsening has progressed as a result of a direct application of Laplace's pressure law in two dimensions by John von Neumann.[16] Adjacent cells generally have different internal pressures, and the pressure difference will induce the diffusion of embedded gas and an increase in the average cell size, known as foam coarsening (see figure 8). The rate of change of a cell area A is determined exactly from its number of sides n: $dA/dt = \alpha(n-6)$.

Surface tension, together with a solubility parameter of the gas in the liquid, is hidden in the lumped coefficient α. Generalizing that result to 3D foams has been recently explored by Sascha Hilgenfeldt and colleagues.[17] There is no strict "von Neumann's law" in 3D because there are too many topological degrees of freedom. The mechanisms of foam coarsening remain, however, an open issue in both two and three dimensions.

Future directions

Capillary phenomena, as noted very early by Newton, have the distinguished feature of being rooted at a very small scale (molecular separations) yet having consequences at macroscopic scales (typically a few millimeters under normal gravity, and much larger scales under microgravity). Progress on the subject has been made by jumps, sometimes huge, as was the one made by Laplace and Young 200 years ago. The jumps were all the result of a combination of precise—and sometimes difficult—experiments and deep thinking. Static problems are now understood, down to the minute details of the density profile across the interface. The frontier nowadays has shifted to nonequilibrium situations—such as the dynamical interaction between a liquid–vapor interface and a solid, and the effects of soluble surfactants in the liquid—and the understanding of broadly distributed properties, such as those found in sprays and foams. In the same manner that diesel engines and ink-jet printers have revived research on breakup, atomization, and sprays in the last century, unexpected technological innovations, geophysical changes, or biological discoveries will certainly motivate future research in capillarity, at least for the next 200 years to come.

References

1. I. Newton, *Opticks*, printed for S. Smith and B. Walford, London (1704).
2. T. Young, *Proc. Roy. Soc.* **95**, 65 (1805).
3. P.-S. Laplace, *Traîté de mécanique céleste*, Courcier, Paris (1805).
4. J. S. Rowlinson, *Cohesion*, Cambridge U. Press, New York (2002).
5. J. C. Maxwell, in *Encyclopedia Britannica* **9**, 541 (1876).
6. L. Mahadevan, Y. Pomeau, *Phys. Fluids* **11**, 2449 (1999); P. Aussillous, D. Quéré, *Nature* **411**, 924 (2001).
7. P. G. de Gennes, *Rev. Mod. Phys.* **57**, 827 (1985).
8. H. A. Stone, L. Limat, S. K. Wilson, J. M. Flesseles, T. Podgorski, *Comptes Rendus Physique* **3**, 103 (2002); M. Ben Amar, L. J. Cummings, Y. Pomeau, *Phys. Fluids* **15**, 2949 (2003).
9. H. A. Stone, A. D. Stroock, A. Adjari, *Annu. Rev. Fluid Mech.* **36**, 381 (2004); T. M. Squires, S. R. Quake, *Rev. Mod. Phys.* **77**, 977 (2005).
10. E. Mariotte, *Traité du mouvement des eaux et des autres corps fluides*, E. Michallet, Paris (1686); F. Savart, *Ann. Chim. (Paris)* **53**, 337 (1833).
11. J. Plateau, *Statique expérimentale et théorique des liquides soumis aux seules forces moléculaires*, Gauthier-Villars, Paris (1873).
12. L. Rayleigh, *Proc. Lond. Math. Soc.* **10**, 4 (1878).
13. J. Eggers, *Rev. Mod. Phys.* **69**, 865 (1997).
14. M. Moseler, U. Landman, *Science* **289**, 1165 (2000).
15. E. Villermaux, P. Marmottant, J. Duplat, *Phys. Rev. Lett.* **92**, 074501 (2004).
16. J. von Neumann, in *Metal Interfaces*, American Society for Metals, Cleveland (1952), p. 108.
17. S. Hilgenfeldt, A. M. Kraynik, S. A. Koehler, H. A. Stone, *Phys. Rev. Lett.* **86**, 2685 (2001).
18. F. E. C. Culick, *J. Appl. Phys.* **31**, 1128 (1960); N. Bremond, E. Villermaux, *J. Fluid Mech.* **549**, 273 (2006). ∎